Small Changes in the Primary Structure of Transportan 10 Alter the Thermodynamics and Kinetics of its Interaction with Phospholipid Vesicles†

Lindsay E. Yandek, Antje Pokorny, and Paulo F. F. Almeida*

Department of Chemistry and Biochemistry, University of North Carolina Wilmington, Wilmington, North Carolina 28403

Received November 4, 2007; Revised Manuscript Received December 24, 2007

ABSTRACT: The kinetics and thermodynamics of binding of transportan 10 (tp10) and four of its variants to phospholipid vesicles, and the kinetics of peptide-induced dye efflux, were compared. Tp10 is a 21-residue, amphipathic, cationic, cell-penetrating peptide similar to helical antimicrobial peptides. The tp10 variants examined include amidated and free peptides, and replacements of tyrosine by tryptophan. Carboxy-terminal amidation or substitution of tryptophan for tyrosine enhance binding and activity. The Gibbs energies of peptide binding to membranes determined experimentally and calculated from the interfacial hydrophobicity scale are in good agreement. The Gibbs energy for insertion into the bilayer core was calculated using hydrophobicity scales of residue transfer from water to octanol and to the membrane/water interface. Peptide-induced efflux becomes faster as the Gibbs energies for binding and insertion of the tp10 variants decrease. If anionic lipids are included, binding and efflux rate increase, as expected because all tp10 variants are cationic and an electrostatic component is added. Whether the most important effect of peptide amidation is the change in charge or an enhancement of helical structure, however, still needs to be established. Nevertheless, it is clear that the changes in efflux rate reflect the differences in the thermodynamics of binding and insertion of the free and amidated peptide groups.

We have recently reported a detailed investigation (*1*) of the mechanism of the interaction of the cell-penetrating peptide (CPP[1]) transportan 10 (tp10) (*2, 3*) with phospholipid membranes. The kinetics of tp10 binding to lipid vesicles and carboxyfluorescein (CF) efflux induced by tp10 from the vesicle lumen could be described by a simple model. In this model, the peptides bind to the vesicle surface and their accumulation creates a mass imbalance across the bilayer. This produces a perturbation that enables tp10 monomers to translocate to the inner surface of the membrane. The presence of peptides in the bilayer renders it permeable to the encapsulated dye, which is released in a graded manner, concomitantly with peptide translocation. When the concentration of tp10 bound to both leaflets of the bilayer is equal, efflux essentially stops because the mass imbalance strain is relieved, and the membrane is no longer perturbed (*1*). Recent molecular dynamics simulations are consistent with this model (*4–6*).

The mechanism of CPPs is a topic of intense research because of their potential use as drug-delivery systems or to transport large cargo into cells, such as DNA or proteins (*7*). Tp10 is a 21-residue, amphipathic peptide constructed from the 14-residue mastoparan from wasp (*Vespula lewisii*) venom, and a 6-residue sequence from the neuropeptide galanin, connected through an additional lysine residue. Tp10 has been shown to transport cargo across cell membranes (*3*). The parent transportan, which is slightly longer than tp10, has been reported to transport even large molecules, such as green fluorescent protein, attached to the peptide through a biotinyl linkage (*8*). Neither tp10 nor transportan function as ligands for the galanin receptor (*2*), suggesting that a direct interaction with the lipid bilayer is involved. Transportan (*9*), *V. lewisii* mastoparan (*10*), and mastoparan X (*11–13*), which are very similar, form amphipathic α-helices when bound to membranes. Therefore, it is very likely that tp10, which is longer than the mastoparans but shorter than transportan, will also form an α-helix under those conditions.

While it appears that in many cases endocytic transport is involved, this does not exclude the possibility of passive translocation across the membrane by CPPs. The values of the Gibbs energies for tp10 binding to the membrane interface and translocating across the bilayer hydrophobic interior suggest that a passive translocation is entirely plausible and requires relatively small changes in bilayer structure (*1*). Transfer of an amphipathic peptide to the bilayer interior may well be more favorable than expected from thermodynamics of transfer from water to octanol (*14*), because binding of many peptides to the membrane will disturb it significantly, increasing the likelihood that some peptides permeate the bilayer. The lipid bilayer is not simply a hydrophobic slab (*14*) and the lipid molecules will respond to the changes caused by binding of a large amount of amphipathic peptides to the membrane surface. A possible adaptive response of the bilayer is the development of positive curvature strain, which has been proposed to be an important component of the mechanism of cytolytic and antimicrobial peptides (*15–18*) that follow the toroidal hole model (*19–21*), the sinking-raft model (*22, 23*), or models involving less-structured pores (*24*). In fact, the structural similarity between the amphipathic class of CPPs, which

† This work was supported in part by National Institutes of Health Grant GM072507.

* To whom correspondence should be addressed. Tel: (910) 962-7300. Fax: (910) 962-3013. E-mail: almeidap@uncw.edu.

10.1021/bi702205r CCC: $40.75
Published on Web 02/09/2008

includes tp10, and antimicrobial peptides (*25*) indicates that many mechanistic aspects may be common to both fields.

Here, we examine the effect of very small variations in the tp10 sequence on the affinity of these peptides for membranes and on their ability to cause leakage from vesicles. Some of the changes involve the alteration of the peptide charge. Therefore, we also investigate the effect of electrostatics more extensively by varying the membrane composition. Membranes based on phosphatidylcholine (PC) are modified by adding phosphatidylglycerol (PG) or phosphatidylserine (PS), to determine the effect of anionic lipid and its specificity. The results are compared with calculated values of the Gibbs energies of binding to the membrane interface and transfer to the membrane interior using the approach of White and Wimley (*14*).

MATERIALS AND METHODS

Materials. 1-Palmitoyl-2-oleoyl-sn-glycero-3-phosphocholine (POPC)[1], 1-palmitoyl-2-oleoyl-sn-glycero-3-phosphoserine (POPS), 1-palmitoyl-2-oleoyl-sn-glycero-3-phosphatidylethanolamine (POPE), and 1-palmitoyl-2-oleoyl-sn-glycero-3-[phospho-rac-(1-glycerol)] (POPG), in chloroform solution, were purchased from Avanti Polar Lipids (Alabaster, AL), Inc. Carboxyfluorescein (99% pure, lot A015252901) was purchased from ACROS (Morris Plains, NJ), 7-methoxycoumarin-3-carboxylic acid (7MC) from Molecular Probes/Invitrogen (Carlsbad, CA), anisole from Aldrich, thioanisole from Alfa Aesar (Ward Hill, MA), and trifluoroacetic acid (TFA) from Mallenckrodt (Phillipsburg, NJ). Organic solvents (HPLC/ACS grade) were purchased from Burdick & Jackson (Muskegon, MI). Lipids and probes were tested by TLC and used without further purification. Fmoc-protected amino acids and resins used in the synthesis of tp10 and its variants were obtained from EMD Biosciences (San Diego, CA).

Synthesis of Lipid Fluorescent Probes. The synthesis of the lipid fluorescent probe 7MC-POPE was performed as previously described in detail (*26, 27*), according the general method of Vaz and Hallmann (*28*).

Preparation of Tp10. Tp10 and its variants were prepared by solid-state synthesis using Fmoc chemistry, on a 0.1-mmol scale, using a PS3 Peptide Synthesizer (Protein Technologies, Inc.), as previously described (*1*). Peptide purity and mass was confirmed with electrospray-ionization time-of-flight (ESI-TOF) mass spectrometry. Tp10–7MC was synthesized for our previous work (*1*) by Dr. Anders Floren from Prof. Ulo Langel's laboratory (Stockholm University, Sweden), who collaborated with us on that publication.

Preparation of Large Unilamellar Vesicles (LUVs). LUVs were prepared by mixing the appropriate lipid amounts in chloroform, in a round-bottom flask; the solvent was rapidly evaporated using a rotary evaporator (Büchi R-3000, Flawil, Switzerland) at 60–70 °C. The lipid film was then placed under a vacuum for 4–8 h and hydrated by the addition of buffer containing 20 mM MOPS, pH 7.5, 0.1 mM EGTA, 0.02% NaN_3, and 100 mM KCl, or appropriately modified as indicated below. The suspension of multilamellar vesicles was subjected to five freeze–thaw cycles to increase the degree of CF encapsulation. The suspension was then extruded 10 times through two stacked Nuclepore polycarbonate filters of 0.1 μm pore size, using a water-jacketed high-pressure extruder from Lipex Biomembranes, Inc. (Vancouver, Canada) at room temperature. Lipid concentrations were assayed by the Bartlett phosphate method (*29*), modified as previously described (*22*).

Efflux Kinetics of Carboxyfluorescein from Lipid Vesicles. LUVs for CF efflux kinetics measurements were prepared by hydration of the lipid film in 20 mM MOPS buffer, pH 7.5, containing 0.1 mM EGTA, 0.02% NaN_3, and 50 mM CF, to yield a final lipid concentration of 10 mM. Following extrusion, LUVs containing CF were passed through a Sephadex-G25 column to separate the dye in the external buffer from the vesicles. For fluorescence measurements, the suspension was diluted to the desired lipid concentration in buffer containing 20 mM MOPS, pH 7.5, 100 mM KCl, 0.1 mM EGTA, and 0.02% NaN_3, which has the same osmolarity as the CF-containing buffer. The kinetics of carboxyfluorescein efflux, measured by the relief of self-quenching of CF fluorescence, were recorded in an Applied Photophysics SX.18MV stopped-flow fluorimeter. The excitation was at 470 nm and the emission was recorded through a long-pass filter OG-530 (Edmund Industrial Optics). For the slower curves, an SLM Aminco 8100 spectrofluorimeter was used, with emission at 520 nm. The peptide concentration was 0.5 μM in all experiments. The fraction of CF release was determined by comparing the final fluorescence with that obtained after addition of Triton-X-100, which dissolves the vesicles and releases all the dye.

The experimental data of CF efflux kinetics were analyzed by calculating the mean lifetime τ of the dye-filled vesicles (*30, 31*). This is defined by (*32, 33*)

$$\tau = \int \frac{dF(t)}{dt} t\, dt \Big/ \int \frac{dF(t)}{dt}\, dt \qquad (1)$$

where $F(t)$ is the experimental fluorescence increase as a function of time, t, due to CF efflux. The apparent mean rate constant is given by $k_{eflx} = 1/\tau$. This is equivalent to an amplitude-weighted average of the apparent time constants in a multiexponential decay (*27*).

Kinetics of Tp10 Binding to Membranes. The kinetics of association of tp10W and tp10W-COOH with LUVs were measured, as previously described (*1, 27*), using fluorescence resonance energy transfer (FRET) from the Trp residue on the peptide to 7MC-POPE incorporated in the membrane, which emits maximally at 396 nm. The data were recorded on an Applied Photophysics SX.18MV stopped-flow fluorimeter, with excitation at 280 nm, and emission measured

[1] Abbreviations: POPC, 1-palmitoyl-2-oleoyl-sn-glycero-3-phosphocholine; POPS, 1-palmitoyl-2-oleoyl-sn-glycero-3-phosphoserine; POPE, 1-palmitoyl-2-oleoyl-sn-glycero-3-phosphatidylethanolamine; POPG, 1-palmitoyl-2-oleoyl-sn-glycero-3-[phospho-rac-(1-glycerol)]; PC, phosphatidylcholine; PS, phosphatidylserine; PG, phosphatidylglycerol; CF, carboxyfluorescein; 7MC, 7-methoxycoumarin-3-carboxylic acid; P/L, peptide/lipid ratio; TFA, trifluoroacetic acid; HPLC, high performance liquid chromatography; LUV, large unilamellar vesicle; CPP, cell-penetrating peptide; ACS, American Chemical Society; ΔG_{if}°, Gibbs energy of peptide binding to the membrane/water interface as a helix; ΔG_{bu}°, Gibbs energy of peptide binding to the membrane/water interface in an unfolded state; ΔG_{bf}°, Gibbs energy of peptide folding to an α-helix on the interface; ΔG_{f}°, Gibbs energy of binding folding to an α-helix in water; ΔG_{oct}°, Gibbs energy of transfer of the peptide from water to the bilayer interior (octanol); $\Delta G_{oct\text{-}if}^{\circ} = \Delta G_{oct}^{\circ} - \Delta G_{i}^{\circ}$; ΔG_{i}° Gibbs energy of transfer of the peptide from the interface to the membrane interior; k, on-rate constant; k, off-rate constant; K_D, equilibrium dissociation constant; τ, efflux lifetime; k, apparent binding rate constant; k, apparent efflux rate constant.

through a long-pass filter GG-385 (Edmund Industrial Optics, Barrington, NJ). The peptide concentration was 0.5 μM and the lipid concentration varied between 25 and 400 μM, both after mixing.

The kinetics of binding were analyzed as previously described in detail (*1, 27*). The concentration (P_L) of peptide bound to lipid vesicles (L) increases over time as a simple exponential

$$P_L(t) = A_o[1 - \exp(-k_{app}t)], \quad (2)$$

where A_o is a constant and

$$k_{app} = k_{on}[L] + k_{off} \quad (3)$$

Here, [L] is the vesicle concentration, but it will always be expressed in terms of lipid concentration. (Because the vesicles have a diameter of about 0.1 μM and the area of a PC molecule is about 0.7 nm^2, 1 LUV $\simeq 1 \times 10^5$ lipids.) Because the number of peptides bound per vesicle is always small and vesicles do not disappear when peptides bind, [L] is considered constant in the calculations.

In the dissociation kinetics experiment (*27*), peptide initially bound to donor vesicles dissociates and irreversibly binds to acceptor vesicles. The donors are vesicles of POPC or POPC/POPS containing 7MC-POPE, whereas the acceptors are pure POPS without fluorescent probes. Irreversible peptide binding to the acceptors is assumed because the affinity of tp10 for pure POPS is much greater than for POPC or POPC/POPS mixtures, and the acceptors are in excess. Under these experimental conditions, the concentration of peptide bound to the donors follows an exponential decay function with a main apparent rate constant that is very close to the true k_{off} (*27*)

$$P_L(t) \simeq A_1 \exp(-k_{off}t) \quad (4)$$

where A_1 is a constant. The change in $P_L(t)$ parallels the decay in fluorescence (FRET) as a function of time, which is measured experimentally.

RESULTS

Carboxyfluorescein Efflux Kinetics. We recently examined the interaction of tp10 with phospholipid bilayers (*1*). One of the major tools in that investigation was the measurement of efflux rates of carboxyfluorescein (CF) encapsulated at high concentration in phospholipid vesicles. Initially CF is self-quenched, but addition of peptide to the vesicles causes CF to escape to the external solution, with a concomitant large increase in fluorescence, which allows monitoring of the kinetics. The goal of that work was to understand the mechanism of bilayer perturbation by tp10, and a detailed model was proposed that described the experimental kinetics very well (*1*).

The investigation reported here was prompted by a striking observation. When the activity of the nonamidated variant of tp10 (tp10-COOH) was examined on POPC vesicles, it was observed that the CF efflux rate decreased dramatically (Figure 1) in comparison with that induced by tp10 (which is amidated at the C-terminus (Table 1)). Amidation eliminates the negative charge of the carboxylate group. Is that single charge difference between tp10 and tp10-COOH responsible for the dramatic change observed in the efflux kinetics? Previously, we had monitored efflux induced by

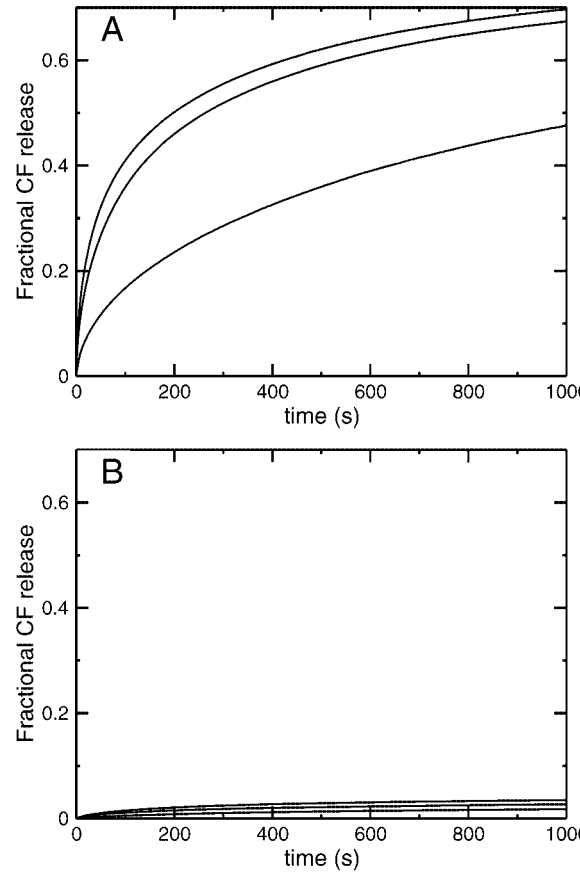

FIGURE 1: CF efflux kinetics from POPC vesicles induced by (A) tp10 and (B) tp10-COOH. The peptide concentration is 0.5 μM and the lipid concentrations are 30, 50, and 100 μM in both panels, 30 being the fastest and 100 μM the slowest curve. The tp10 data (A) are from Yandek et al. (*1*) The curves are normalized by the Triton level, which is a horizontal line at 1.0.

tp10 from POPC vesicles, which are neutral, and POPS/POPC 20:80 vesicles, which are anionic. Although tp10 has a +5 charge at neutral pH, its activity toward the two types of vesicles was similar (*1*). Therefore, we decided to examine in more detail the effects of electrostatics on efflux kinetics and membrane binding, by varying the charge on the lipid membrane.

CF efflux kinetics were examined in mixtures of POPS/POPC and POPG/POPC, with 20:80 and 50:50 compositions, to determine the importance of membrane charge for activity and whether the specific nature of the anionic lipid matters, by comparing POPS and POPG. The results are shown in Figure 2. As before, a strong dependence on the peptide/lipid ratio (P/L) is observed, efflux becoming faster at higher peptide concentration on the membrane. Membrane negative charge can rescue the activity of tp10-COOH significantly, but the nature of the anionic lipid does not seem to matter much: when the vesicles contain POPG or POPS the efflux induced by tp10-COOH occurs over similar time scales. The question that begs to be answered is whether these effects are simply a consequence of differences in peptide binding.

The binding results are described in the next section, but we also examined efflux kinetics induced by three additional tp10 variants (tp10W, tp10W-COOH, and tp10–7MC), although not to the same extent as for tp10-COOH (and previously for tp10). Table 1 lists the sequences and charges of the five tp10 variants. Table 2 summarizes the efflux

Table 1: Peptide Sequences and Charge at pH 7.5

peptide	sequence	net charge	no. of charges
tp10	AGYLLGKINLKALAALAKKIL-NH_2	+5	5
tp10-COOH	AGYLLGKINLKALAALAKKIL	+4	6
tp10W	AGWLLGKINLKALAALAKKIL-NH_2	+5	5
tp10W-COOH	AGWLLGKINLKALAALAKKIL	+4	6
tp10–7MC	AGYLLGK(−7MC)INLKALAALAKKIL-NH_2	+4	4

kinetics for experiments where the peptide final concentration is 0.5 μM and the lipid concentration is 30 μM (after mixing in the stopped-flow system). The rate of efflux is characterized here by a model-free parameter, the lifetime τ for CF release from the vesicles, which is related to the mean apparent efflux rate constant by $k_{eflx} = 1/\tau$. We observe very significant differences between the five tp10 variants, which cause efflux in the following order, from fastest to slowest, tp10–7MC > tp10W > tp10 > tp10W-COOH > tp10-COOH.

Tp10 Binding to Phospholipid Bilayers: Kinetics and Equilibrium. Tp10 and tp10-COOH do not have a tryptophan. Previously, we used tp10–7MC, a version of tp10 modified with the fluorophore 7-methoxycoumarin-4-acetic acid, to measure binding to membranes (*1*). This fluorophore is attached to the ϵ-amino group of Lys-7 of tp10 through an amide bond to the acetic acid group of the coumarin. Thus, a positive charge is eliminated in tp10–7MC in comparison with tp10. Here, two additional variants were synthesized, tp10W and tp10W-COOH, containing a Trp residue instead of Tyr at position 3 of tp10, to enable measurement of binding to membranes. The kinetics of tp10–7MC binding to POPC and POPS/POPC were previously reported (*1*). Now, to measure binding of tp10W and tp10W-COOH to phospholipid vesicles, we incorporated into the membrane 1 mol% lipid fluorophore 7MC-POPE, which acts as a fluorescence resonance energy transfer (FRET) acceptor for the Trp on the peptide (*27*). If Trp is excited at 280 nm, a significant increase in 7MC-POPE fluorescence emission at 396 nm occurs upon peptide binding. The kinetics tp10W and tp10W-COOH binding to POPC and POPS/POPC mixtures were measured at room temperature (~22 °C) by monitoring the rate of change in fluorescence emission of 7MC-POPE by stopped-flow fluorescence. Examples are shown in panels A and D in Figure 3 for POPC and POPS/POPC 50:50, respectively. In most cases, the fluorescence intensity curves as a function of time were well fit by a single exponential rise (eq 2). The apparent rate constant (k_{app}) determined from the fits was plotted as a function of lipid concentration to obtain the on-rate constant (k_{on}), from the slope, and the off-rate constant (k_{off}), from the intercept, as shown in panels B and E in Figure 3 for POPC and POPS/POPC 50:50, respectively. The values obtained for the rate constants are listed in Table 3 for all tp10 variants examined for binding now (tp10W and tp10W-COOH) and previously (tp10–7MC).

In some cases, the intercept occurs too close to the origin to obtain a good estimate of k_{off}; therefore, the dissociation

Table 2: Lifetime of Tp10-Induced CF Efflux from Phospholipid Vesicles[a]

peptide/vesicle composition	CF efflux τ (s^{-1})
Tp10	
POPC	170
POPS/POPC 20:80	40
Tp10-COOH	
POPC	19000
POPS/POPC 20:80	150
POPS/POPC 50:50	30
POPG/POPC20:80	240
POPG/POPC50:50	4
Tp10W	
POPC	30
POPS/POPC 20:80	25
Tp10W-COOH	
POPC	1650
POPS/POPC 20:80	10
Tp10–7MC	
POPC	11
POPS/POPC 20:80	14

[a] The peptide concentration is 0.5 μM and the lipid concentration is 30 μM in all cases listed here. The values of τ are very similar within one vesicle preparation, but the variance between preparations is larger, with standard deviations of about 30–50%.

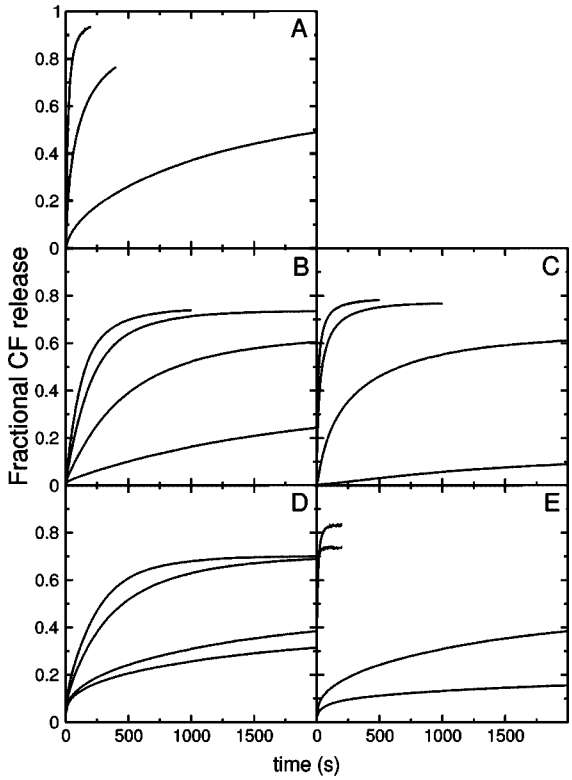

FIGURE 2: Effect of anionic lipid on efflux kinetics. CF efflux induced by (A) tp10 from vesicles of POPS/POPC 20:80, (B) tp10-COOH from POPS/POPC 20:80, (C) tp10-COOH from POPS/POPC 50:50, (D) tp10-COOH from POPG/POPC 20:80, and (E) tp10-COOH from POPG/POPC 50:50. The peptide concentration is 0.5 μM and the lipid concentrations are 30, 50, 100, and 200 μM (not in A), 30 being the fastest and 200 (100 in A) μM the slowest curve. The tp10 data (A) is from. The curves are normalized by the Triton level, which is a horizontal line at 1.0.

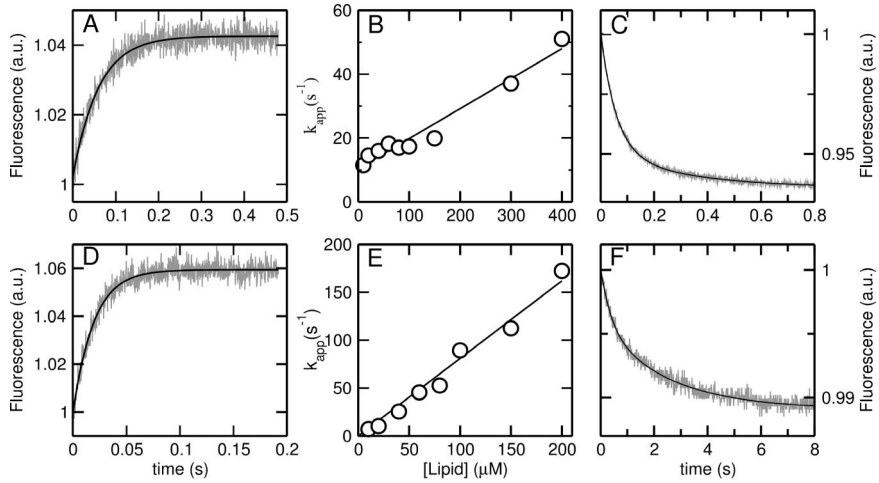

FIGURE 3: Binding and dissociation kinetics of tp10W for (A−C) POPC and (D−F) POPS/POPC 50:50. (A, D) Binding kinetics of tp10W (0.5 μM) to lipid vesicles (80 μM lipid). (B, E) Plot of the apparent rate constant (k) from the binding kinetics as a function of lipid concentration to determine k_{on} (slope) and k_{off} (y-intercept). (C, F) Dissociation kinetics of tp10W (0.5 μM) from lipid vesicles (100 μM lipid). In A, C, D, and E, the experimental data are the gray traces; the lines are one-exponential fits in A and D and two-exponential fits in C and F.

Table 3: Kinetic Rate Constants and Equilibrium Dissociation Constants for tp10 Binding to Phospholipid Vesicles

vesicle composition	binding		dissociation k_{off} (s^{-1})	average k_{off} (s^{-1})	equilibrium K_D (μM)
	k_{on} (M^{-1} s^{-1})	k_{off} (s^{-1})			
			Tp10W		
POPC	$(9.4 \pm 0.7) \times 10^4$	10.4 ± 1.3	15 ± 3	12.7 ± 1.6	140 ± 20
POPS/POPC 20:80	$(5.9 \pm 0.4) \times 10^5$	≤ 3		$\sim 2^a$	~ 3
POPS/POPC 50:50	$(8.1 \pm 0.6) \times 10^5$	≤ 3	0.38 ± 0.15	0.4 ± 0.2	0.5 ± 0.2
			Tp10W-COOH		
POPC	$(4.8 \pm 1.3) \times 10^5$	110 ± 30	30 ± 7	100 ± 30	200 ± 50
POPS/POPC 20:80	$(6.9 \pm 0.7) \times 10^5$	14 ± 5	4.3 ± 0.9	9 ± 3	13 ± 4
POPS/POPC 50:50	$(7.2 \pm 0.8) \times 10^5$	≤ 5	0.9 ± 0.3	0.9 ± 0.3	1.2 ± 0.4
			Tp10–7MC[b]		
POPC	$(7.4 \pm 0.5) \times 10^4$	1.5 ± 0.4		1.5 ± 0.4	20 ± 5
POPS/POPC 20:80	$(2.6 \pm 0.08) \times 10^5$	2.4 ± 0.3		2.4 ± 0.3	9 ± 1
POPS/POPC 50:50	$(5.8 \pm 0.8) \times 10^5$	≤ 5		$\sim 2^c$	3.5 ± 1.0

[a] Value estimated from binding and from the dissociation of Tp10W-COOH, which is about twice as fast in all cases. [b] Data from Yandek et al. (*1*). [c] Value estimated on the basis that k_{on} seems to show little dependence on PS content; the uncertainty at the intercept was too high to determine from plot of k_{app} against lipid concentration.

kinetics were measured in a more direct manner, as previously described in detail (*27*). Briefly, peptide was first incubated with vesicles of POPC or POPS/POPC containing 1 mol% 7MC-POPE, and then these vesicles were mixed with an excess of pure POPS vesicles (500 μM). Since the acceptors are in excess and binding to POPS is much stronger, the peptide, after dissociating from the donors into water, is most likely to bind to the acceptors. Thus, dissociation is essentially irreversible, and the kinetics of decrease in fluorescence emission from 7MC-POPE in the donors allow to estimate k_{off} (panels C and F in Figure 3 for POPC and POPS/POPC 50:50). In most cases, the dissociation kinetics were well-described by a single exponential decay. If this did not happen, two exponentials were sufficient to describe the curves and k_{off} was estimated as the reciprocal of the average lifetime (eq 1). The values obtained are listed in Table 3. This table also includes the average value for k_{off} obtained from the two assays (or our best estimate when one of the assays appears more trustworthy), and the equilibrium dissociation constant calculated from k_{on} and the average k_{off}. For tp10W, the results from the two assays agree well. For tp10W-COOH, the k_{off} obtained from the dissociation experiment is systematically smaller than determined from the intercept in the binding experiment. This probably reflects peptide translocation that occurred during the incubation with the donor vesicles; peptides that went inside must cross the membrane again to dissociate and this decreases the apparent k_{off} determined in the dissociation assay. Because of that, we have given more weight to the k_{off} determined from binding experiments with tp10W-COOH, particularly in the case of POPC, which yielded the largest experimental error, and poorest agreement between the two assays.

Thermodynamics of Membrane Binding and Insertion. The interpretation of our experimental results requires an examination of the thermodynamics of tp10 binding to membranes and its possible insertion into the bilayer hydrophobic core. In the model proposed for tp10 (*1*), the peptide monomers bind to the membrane surface, fold into an α-helix, and cross the membrane by inserting into, and perturbing the hydrophobic core of the lipid bilayer. In doing so, they cause graded dye release from the vesicle lumen. Although the lipids are proposed to adapt to some extent to this membrane perturbation (*1*), thus diminishing the unfavorable character of the inserted state, it is instructive to analyze in a simple

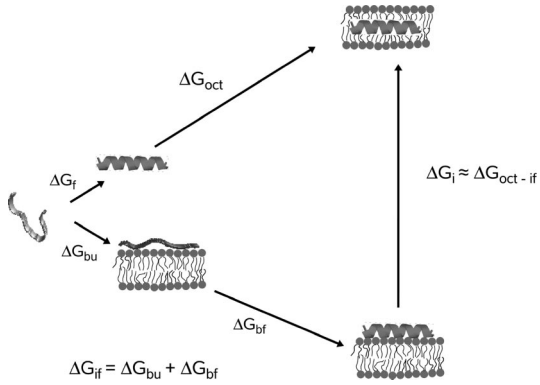

FIGURE 4: Thermodynamic cycle for peptide binding to the membrane and insertion into the bilayer hydrophobic core, modified from the scheme originally presented by Yandek et al. (*1*), with permission of *Biophys. J*.

manner the thermodynamics of peptide transfer to the membrane nonpolar interior. To do this, we use the formalism developed by White and Wimley (*14*), as in our first investigation of tp10 (*1*).

Consider the scheme of Figure 4, which depicts the thermodynamic changes accompanying peptide transfer from water to the membrane interface and to its nonpolar core. Note that this is not a model of the peptide mechanism but a thermodynamic cycle that can be calculated for the processes indicated. The Gibbs energy of peptide binding to the membrane/water interface (ΔG_{if}°) is composed of two terms: ΔG_{bu}°, for binding in an unfolded state, and ΔG_{bf}°, for folding to an α-helix on the interface (*14*). Both of these quantities can be estimated using the interfacial transfer scale (*14, 34*). Insertion of the peptide (ΔG_i°), that is, transfer from the interface to the membrane interior, is a high Gibbs energy step. ΔG_i° can be estimated by closing the thermodynamic cycle of Figure 4, taking into account folding of the peptide in water (ΔG_f°) and its transfer from water to the bilayer interior (ΔG_{oct}°), which is estimated using the octanol transfer scale (*14*) The main uncertainty is the value of the Gibbs energy for folding in aqueous solution, which is probably positive but small; previously an estimate of about +1 kcal/mol was used (*1*). Because this value is small, the Gibbs energy of insertion can be estimated as the difference between the Gibbs energies of transfer from water to the hydrophobic core and to the membrane interface, $\Delta G_i^\circ \approx \Delta G_{oct\text{-}if}^\circ = \Delta G_{oct}^\circ - \Delta G_{if}^\circ$. In reality, the barrier for translocation is probably smaller because the lipids will adapt to the peptide perturbation, but as shown below, the good correlation observed between peptide insertion (ΔG_i°) and dye efflux suggests that the peptide experiences to some extent the nonpolar medium of the bilayer interior.

We have performed the calculations of the various ΔG° using the experimentally based algorithm of Wimley, Hristova, and White (*14, 35*), which is implemented by the program Membrane Protein Explorer (MPEx) (*36*). The results are listed in Table 4 for all tp10 variants. The Gibbs energy of binding to the membrane was also calculated, from our experimental data, using $\Delta G_{if}^\circ = RT \ln (K_D/2) - 2.4$ kcal/mol, where R is the gas constant and T is temperature. K_D ($= k_{off}/k_{on}$) is divided by 2 for the following reason. The values of k_{on} and k_{off} are reported for binding to lipid vesicles, whose concentration is expressed in terms of lipid concentration, with the usual assumption that 1 LUV contains 1×10^5 lipids. This leaves k_{on}, k_{off}, and K_D free of any interpretation regarding the translocation of the peptide across the bilayer, and whether only the top monolayer or both should be considered in calculating the values of those constants. Now, however, we take the view that the peptide, in the time frame of the binding kinetics, associates primarily with the top monolayer of the membrane. With this assumption, only half the lipid should be used in the calculation. The term −2.4 kcal/mol, which equals $-RT \ln 55$, is the so-called cratic correction for the mixing entropy in water when using a molar concentration scale. This correction, though not entirely consensual, has been advocated by White and Wimley (*14*) and we use it here for consistency. As can be seen from Table 4, the calculated and experimental values of the Gibbs energy of binding to POPC (ΔG_{if}°) are in good agreement.

Table 4: Thermodynamics of Peptide Binding and Insertion into Phospholipid Membranes

peptide	membrane	ΔG_{if}° (kcal/mol) experiment[a]	ΔG_{if}° (kcal/mol) calculated[b]	$\Delta G_{oct\text{-}if}^\circ$ (kcal/mol) calculated
Tp10	POPC		−7.8	+19.1
	POPS/POPC 20:80[c]		−10.1	
Tp10-COOH	POPC		−5.8	+20.9
	POPS/POPC 20:80		−8.7	−10.4
	POPS/POPC 50:50		−9.9	
Tp10W	POPC	−8.1	−8.6	+18.6
	POPS/POPC 20:80	−10.4		
	POPS/POPC 50:50	−11.4		
Tp10W-COOH	POPC	−7.9	−6.7	+20.3
	POPS/POPC 20:80	−9.8		
	POPS/POPC 50:50	−11		
Tp10–7MC	POPC	−9.3		+17.5[d]
	POPS/POPC 20:80	−9.7		

[a] Calculated from $\Delta G_{if}^\circ = RT \ln(K_D/2) - 2.4$ kcal/mol. This assumes that in the time frame of the on-rate kinetics the peptides did not translocate across the bilayer; hence, K_D is divided by 2. The −2.4 kcal/mol are the cratic correction as recommended by White and Wimley (*14*). [b] A helical content of 70%, which is a typical value fro this type of peptides, was assumed in the calculation of ΔG_{if}°. [c] For tp10 and tp10-COOH binding to PS/PC mixtures, the value of ΔG_{if}° was calculated assuming that K_D decreases from the theoretical value for POPC by the same factor as observed experimentally for tp10W and tp10W-COOH, respectively. [d] This value is only a rough estimate. It is based on using for the Lys-7MC residue the values given for Tyr by White and Wimley (14); the rationale for using Tyr as a mimic is that the experimental value for ΔG_{if}° for tp10–7MC is almost identical to the theoretical ΔG_{if}° for a tp10 variant where Lys-7 is replaced by Tyr.

The theoretical values of ΔG_{if}° for binding of tp10 and tp10-COOH to mixtures of POPS/POPC cannot be determined from the White and Wimley (*14*) formalism, which applies only to POPC. They can, however, be estimated using the calculated value for POPC modified by adding a term identical to the difference observed experimentally in ΔG_{if}° between POPC and the mixture in question for the peptides tp10W and tp10W-COOH. Thus, the assumption is that the differential enhancement in binding caused by anionic lipid is the same for peptides that differ only in the substitution of Trp for Tyr. Namely, the effect of anionic lipid should be similar on tp10 and tp10W, and should be similar on tp10-COOH and tp10W-COOH. Finally, the value of $\Delta G_{oct\text{-}if}^\circ$ for tp10–7MC is also not available, not even for POPC, because residue 7 of this peptide is Lys-amide-methoxycoumarin, for which no transfer thermodynamic data are available. The value listed is only a rough estimate based on the observation that the Gibbs energy for binding to the interface determined

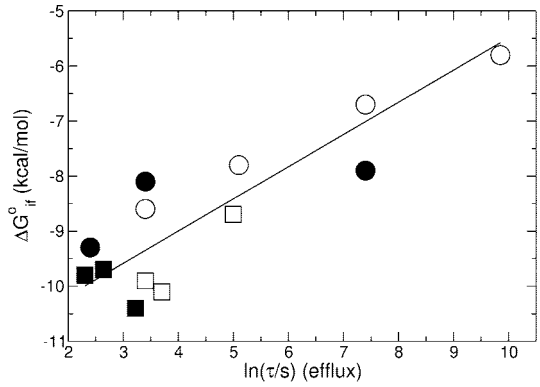

FIGURE 5: Correlation between the Gibbs energy of binding of tp10 variants to the membrane interface (ΔG_{if}°) and the logarithm of the efflux lifetime, τ (in seconds). Solid symbols correspond to experimental values and open symbols to calculated values of ΔG°. Circles correspond to POPC vesicles and squares to POPS/POPC. The line has a slope of 0.568 kcal/mol, which is *RT* at room temperature. The efflux τ is for experiments with 0.5 μM peptide and 30 μM lipid in all cases.

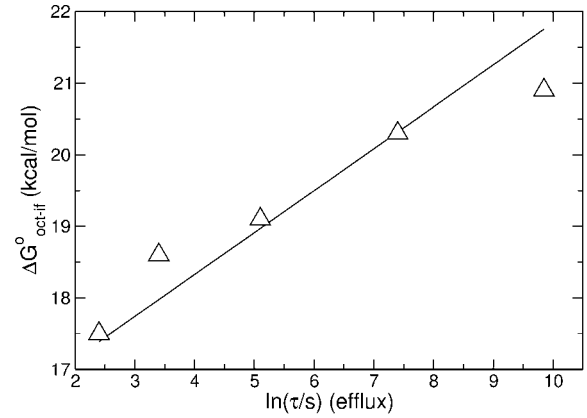

FIGURE 6: Correlation between the calculated Gibbs energy of insertion into the POPC bilayer core ($\Delta G_{oct\text{-}if}^{\circ}$) and the logarithm of the efflux lifetime, τ (in seconds). The line has a slope of 0.568 kcal/mol, which is *RT* at room temperature. The efflux τ is for experiments with 0.5 μM peptide and 30 μM lipid in all cases.

experimentally ($\Delta G_{if}^{\circ} = -9.3$ kcal/mol) is very close to the calculated value for tp10 if Lys-7 is replaced by a Tyr ($\Delta G_{if}^{\circ} = -9.7$ kcal/mol). We conjecture that the transfer to octanol will also be similar and so will be their difference, $\Delta G_{oct\text{-}if}^{\circ}$. The estimate for binding of tp10–7MC to POPS/POPC was calculated in the same manner as for tp10 and tp10-COOH.

Correlation between Binding, Insertion, and Efflux. Let us consider the correlation between peptide binding, insertion, and CF efflux for all tp10 variants. Figure 5 shows experimental (solid symbols) and calculated (open symbols) Gibbs energies of peptide binding (ΔG_{if}°) plotted against the logarithm of the efflux lifetime (ln τ). For POPC (circles), ΔG_{if}° increases monotonically as τ increases. The line shown has a slope of *RT* (0.586 kcal/mol at 22 °C), which is what is expected from the general relation between an equilibrium constant (*K*) and a Gibbs energy ($\Delta G^{\circ} = -RT \ln K$). For POPS/POPC mixtures (squares), binding is much more favorable, with $\Delta G_{if}^{\circ} \approx -10$ kcal/mol for all peptides, and efflux is fast (small τ). However, the correlation between ΔG° and τ is poorer. This is probably because the electrostatic and hydrophobic components of peptide binding to membranes are not exactly additive (*37*). In fact, our values are very similar to those obtained by Ladokhin and White (*37*), which are also mainly clustered at about −9 to −11 kcal/mol for binding of variants of the antimicrobial peptide indolicidin to POPC/POPG vesicles containing between 20 and 100% POPG.

Figure 6 shows calculated Gibbs energies of insertion ($\Delta G_{oct\text{-}if}^{\circ}$) plotted against the logarithm of the efflux lifetime. Again, the line shown has a slope of *RT* because this is also what is expected in general for the relation between a rate constant (*k*) and a Gibbs activation energy ($\Delta G^{\ddagger} \sim -RT \ln k$). Because $\Delta G_{oct\text{-}if}^{\circ}$ corresponds to the highest intermediate in the thermodynamic cycle (Figure 4) it should be close to the activation energy, according to Hammond's (*38*) postulate. From these data, it is not possible to decide whether the efflux rate is determined primarily by binding or insertion, because these thermodynamic changes vary in parallel, as the same energetic considerations affect both, albeit to different degrees (*14*). However, using the pair tp10W/tp10W-COOH as a guide, the effect of amidation on k_{on} and k_{off} is not sufficient to bring the curves for efflux from POPC vesicles induced by tp10 onto the curves induced by tp10-COOH (Figure 1). Therefore, it is likely that contributions from both ΔG_{if}° and $\Delta G_{oct\text{-}if}^{\circ}$ be involved, as suggested by the correlations with efflux.

DISCUSSION

General Framework. Five variants of the CPP tp10 were compared regarding peptide-induced CF efflux from lipid vesicles, and the kinetics and thermodynamics of binding to membranes. These experiments were performed as a function of membrane composition, using POPC as reference. The consequences of replacing some of the POPC by an anionic lipid and the effect of the nature of this lipid were also examined. The primary structures of the peptide variants had only minor differences relative to each other. This comprises versions with amidated and free carboxylic C-termini, a version in which one internal Lys was modified through an amide linkage to a fluorescent moiety, and variants where an aromatic residue, Tyr, was replaced by a more hydrophobic one, Trp.

In spite of the small changes in peptide structure, dramatic effects on their binding to POPC and efflux induced from those vesicles resulted. Simple amidation of the C-terminus or amidation of an internal Lys with a fluorophore both resulted in faster peptide-induced efflux (smaller efflux τ, Table 2). Those amidations eliminate a negative (C-terminus) or a positive charge (internal Lys). We interpret these results in view of the model we previously proposed for tp10 (*1*), in which peptide monomers bind to the membrane and permeate it, perturbing the membrane and inducing dye release from the vesicle lumen. Although helped by lipid rearrangement, possibly with some induced local curvature, translocation was proposed to involve a significant exposure of the peptide to the nonpolar region of the bilayer. The translocation step across a nonpolar medium explains the effect of peptide modification on CF efflux: it is thermodynamically easier to place in the bilayer interior an amidated C-terminus or a fluorophore-amidated Lys residue than their charged, nonamidated counterparts (*35*).

Effect of Membrane Charge. Peptide binding is significantly enhanced by increasing the content of anionic lipids in POPC vesicles. The inclusion of anionic lipids in the

membrane lowers the binding Gibbs energy by about 2 kcal/mol from POPC to POPS/POPC 20:80, and by an extra 1 kcal/mol to POPS/POPC 50:50, for tp10W (charge of +5) and tp10W-COOH (+4), but not for tp10–7MC (+4), which already binds very well to POPC. This shows the nonadditivity of electrostatic and hydrophobic interactions in peptide binding to membranes, which has been demonstrated by Ladokhin and White (*37*). Concomitantly with better binding to anionic vesicles, the efflux rate increases in most tp10 variants. The Gibbs energy of the peptide in the interior of anionic bilayers is likely to remain similar to that in POPC. Therefore, if the Gibbs energy of the peptide bound to the interface decreases when binding improves, we would expect the transfer to the bilayer interior from the interface to become more unfavorable, which would slow down translocation and efflux. However, this is not observed, suggesting that some of the binding energy is used to disturb the bilayer, making the inserted state more favorable. This may involve local curvature, keeping some lipid headgroups in contact with the peptide.

Effect of C-Terminal Amidation. The rate of efflux from POPC vesicles is dramatically lower in nonamidated (free C-terminal carboxylate) versions than in C-terminal-amidated versions of tp10 (Figure 1 and Table 2). To some extent, this can be compensated by the charge on the membrane: if the anionic lipid content is increased, binding and efflux induced by the terminal-COOH versions approach those induced by the C-terminal-amidated versions of tp10. This is because binding is then driven to a significant extent by electrostatics and all peptides are cationic overall (+4 or +5). The effect of amidation on peptide activity has not been much investigated. Early work indicated that the C-terminal-amidated version of the antimicrobial peptide sarcotoxin IA was more effective than its free carboxylate counterpart, both with regard to bacteria and model membranes (*39*). Also, comparison of free and C-terminal-amidated versions of the 1–18 amino terminal fragment of dermaseptin indicated that the amidated version was a more potent antimicrobial, but devoid of hemolytic activity (*40*). However, free carboxylate and terminal-amidated versions of clavanin A behave very similarly (*41*), whereas replacing the terminal carboxylate of pardaxin with an amine derivative with a +4 charge, significantly increases its antimicrobial potency (*42*). More recently, C-Terminal amidation of dermaseptin S3 was shown to lead to formation of a small region of α-helical structure (13%) where none existed (*43*), but the significance of this slight change for activity has not been established. C-Terminal amidation of tritrpticin resulted in only a moderate increase in antimicrobial activity, by a factor of about 2 (*44*). Taken together, those results seem to indicate that C-terminal amidation renders peptides somewhat more effective. This is consistent with the thermodynamics of converting the C-terminal carboxylate to an amide: amidation increases binding to the POPC interface, with a change in Gibbs energy of −1.9 kcal/mol, and it enhances partitioning into nonpolar media (octanol), with a change in Gibbs energy of −3.6 kcal/mol (*35*). Both effects are likely to lead to peptides with higher activity.

Thermodynamics of Peptide Transfer. The thermodynamic analysis of transfer of peptides from water to the POPC membrane interface (binding) and from the interface to the bilayer hydrophobic interior (insertion), using the interfacial and octanol transfer scales of White and Wimley (*14*), provides a very simple way to understand the effect of amidation of the C-terminus or an internal Lys residue on peptide activity. For the tp10 variants examined, both the Gibbs energy of binding (experimental and calculated) and the Gibbs energy of insertion are clearly correlated with the lifetime τ for CF efflux from POPC vesicles (Figures 5 and 6). How much the effect of amidation on binding and insertion is due to electrostatics remains to be established. On the one hand, amidation is known to stabilize the α-helical structure, and structuring has been shown to increase activity of antimicrobial peptides (*45, 46*) that are similar to amphipathic CPPs. On the other hand, transfer of a charge on a peptide to the POPC interface is associated with a significant Gibbs energy cost: about 1 kcal/mol for His^+, Lys^+, and Arg^+; and 1.2 to 2 kcal/mol for Asp^- and Glu^- (*14*). In the case of tp10 variants, as the total number of charges−positive plus negative−on the peptide decreases from 6 to 5 and to 4, the Gibbs energy of binding (ΔG_{if}°) becomes more negative (Table 4). Transfer of a charge on the peptide to the bilayer hydrophobic core is associated with an even greater Gibbs energy cost (*14*), which impairs insertion and translocation. As the total number of charges in tp10 variants increases, the Gibbs energy of insertion (ΔG_i°) into POPC also increases (Table 4). As is well-known, increasing the number of positive charges enhances the activity of antimicrobial peptides on anionic vesicles and bacteria and the translocation of CPPs, but only up to a point. Eventually, an optimum number of positive charges is reached and further increase in charge results in a decrease in activity. The optimal charge varies from peptide to peptide, but is typically between +4 to +9 for antimicrobial peptides (*47–49*) and between +7 to +15 for arginine-rich CPPs (*50, 51*). However, binding and activity of antimicrobial peptides on zwitterionic PC vesicles are impaired as the positive charge on the peptide increases (*48*). Our results on tp10 are in agreement with both of those aspects: the improvement arising from positive charge for binding and activity toward anionic vesicles and its detrimental effect on binding and activity toward zwitterionic vesicles. We suggest that the decline in peptide activity toward anionic vesicles and cells when charge is increased beyond the optimum, and the steady decline toward zwitterionic vesicles probably reflects the unfavorable thermodynamics of transfer into the nonpolar region of the membrane, even if mitigated by lipid rearrangement. Although more work is necessary to understand whether the most important effect of peptide amidation is the change in charge or an enhancement of helical structure, it is clear that the changes in efflux rate reflect the differences in the thermodynamics of binding and insertion of the free and amidated peptide groups.

ACKNOWLEDGMENT

We thank Prof. Ulo Langel of Stockholm University, Sweden, for having enticed us to examine tp10, and Dr. Will

Boomershine for assistance in the synthesis of tp10, tp10-COOH, tp10W, and tp10W-COOH.

REFERENCES

1. Yandek, L. E., Pokorny, A., Floren, A., Knoelke, K., Langel, U., and Almeida, P. F. F. (2007) Mechanism of the cell-penetrating peptide transportan 10 permeation of lipid bilayers. *Biophys. J. 92*, 2434–2444.
2. Soomets, U., Lindgren, M., Gallet, X., Hallbrink, M., Elmquist, A., Balaspiri, L., Zorko, M., Pooga, M., Brasseur, R., and Langel, U. (2000) Deletion analogues of transportan. *Biochim. Biophys. Acta 1467*, 165–176.
3. Hällbrink, M., Floren, A., Elmquist, A., Pooga, M., Bartfai, T., and Langel, U. (2001) Cargo delivery kinetics of cell-penetrating peptides. *Biochim. Biophys. Acta 1515*, 101–109.
4. Leontiadou, H., Mark, A. E., and Marrink, S. J. (2006) Antimicrobial peptides in action. *J. Am. Chem. Soc. 128*, 12156–12161.
5. Lopez, C. F., Nielsen, S. O., Srinivas, G., DeGrado, W. F., and Klein, M. L. (2006) Probing membrane insertion activity of antimicrobial polymers via coarse-grain molecular dynamics. *J. Chem. Theory Comput. 2*, 649–655.
6. Nielsen, S. O., Lopez, C. F., Srinivas, G., and Klein, M. L. (2004) Coarse grain models and the computer simulation of soft materials. *J. Phys.: Condens. Matter 16*, R481–R512.
7. Langel, U. (2006), editor. Handbook of Cell-Penetrating Peptides, Boca Raton, FL, 2006 (2nd Ed).
8. Pooga, M., Kut, C., Kihlmark, M., Hällbrink, M., Fernaeus, S., Raid, R., Land, T., Hallberg, E., Bartfai, T., and Langel, U. (2001) Cellular translocation of proteins by transportan. *Faseb J. 15*, 1451–1453.
9. Magzoub, M., Kilk, K., Eriksson, L. E. G., Langel, U., and Gräslund, A. (2001) Interaction and struture induction of cell-penetrating peptides in the presence of phospholipid vesicles. *Biochim. Biophys. Acta 1512*, 77–89.
10. Higashijima, T., Wakamatsu, K., Takemitsu, M., Fujino, M., Nakajima, T., and Miyazawa, T. (1983) Conformational change of mastoparan from wasp venom on binding with phospholipid membrane. *FEBS Lett. 152*, 227–230.
11. Wakamatsu, K., Higashijima, T., Fujino, M., Nakajima, T., and Miyazawa, T. (1983) Tranferred NOE analyses of conformations of peptides as bound to membrane bilayer of phospholipid; mastoparan-X. *FEBS Lett. 162*, 123–126.
12. Todokoro, Y., Yumen, I., Fukushima, K., Kang, S.-W., Park, J.-S., Kohno, T., Wakamatsu, K., Akutsu, H., and Fujiwara, T. (2006) Structure of tightly membrane-bound mastoparan-X, a G-protein-activating peptide, determined by solid-state NMR. *Biophys. J. 91*, 1368–1379.
13. Harada, E., Todokoro, Y., Akutsu, H., and Fujiwara, T. (2006) Detection of peptide-phospholipid interaction sites in bilayer membranes by^{13}C NMR spectroscopy: Observation of 2H/31P-selective 1H-depolarization under magic-angle spinning. *J. Am. Chem. Soc. 128*, 10654–10655.
14. White, S. H., and Wimley, W. C. (1999) Membrane protein folding and stability: Physical principles. *Annu. Rev. Biophys. Biomol. Struct. 28*, 319–365.
15. Wieprecht, T., Dathe, M., Epand, R. M., Beyermann, M., Krause, E., Maloy, W. L., MacDonald, D. L., and Bienert, M. (1997) Influence of the angle subtended by the positively charged helix face on the membrane activity of amphipathic, antibacterial peptides. *Biochemistry 36*, 12869–12880.
16. Matsuzaki, K., Sugishita, K., Ishibe, N., Ueha, Nakata, S., M., Miyajima, K., and Epand, R. M. (1998) Relationship of membrane curvature to formation of pores by magainin 2. *Biochemistry 37*, 11856–11863.
17. Henzler Wildman, K. A., Lee, D.-K., and Ramamoorthy, A. (2003) Mechanism of lipid bilayer disruption by the human antimicrobial peptide, LL-37. *Biochemistry 42*, 6545–6558.
18. Hallock, K. J., Lee, D.-K., and Ramamoorthy, A. (2003) MSI- 78 an analogue of the magainin antimicrobial peptides, disrupts lipid bilayer structure via positive curvature strain. *Biophys. J. 84*, 3052–3060.
19. Matsuzaki, K., Murase, O., Fujii, N., and Miyajima, K. (1996) An antimicrobial peptide, magainin 2, induced rapid flip-flop of phospholipids coupled with pore formation and peptide translocation. *Biochemistry 35*, 11361–11368.
20. Ludtke, S. J., He, K., Heller, W. T., Harroun, T. A., Yang, L., and Huang, H. W. (1996) Membrane pores induced by magainin. *Biochemistry 35*, 13723–13728.
21. Huang, H. W. (2000) Action of antimicrobial peptides: Two-state model. *Biochemistry 39*, 8347–8352.
22. Pokorny, A., Birkbeck, T. H., and Almeida, P. F. F. (2002) Mechanism and kinetics of δ -lysin interaction with phospholipid vesicles. *Biochemistry 41*, 11044–11056.
23. Pokorny, A., and Almeida, P. F. F. (2004) Kinetics of dye efflux and lipid flip-flop induced by δ -lysin in phosphatidylcholine vesicles and the mechanism of graded release by amphipathic, α -helical peptides. *Biochemistry 43*, 8846–8857.
24. Hancock, R. E. W., and Chapple, D. S. (1999) Peptide antibiotics. *Antimicrob. Agents Chemother. 43*, 1317–1323.
25. Zasloff, M. (2002) Antimicrobial peptides of multicellular organisms. *Nature 415*, 389–395.
26. Frazier, M. L., Wright, J. R., Pokorny, A., and Almeida, P. F. F. (2007) Investigation of domain formation in sphingomyelin/cholesterol/POPC mixtures by fluorescence resonance energy transfer and Monte Carlo simulations. *Biophys. J. 92*, 2422–2433.
27. Gregory, S. M., Cavenaugh, A. C., Journigan, V., Pokorny, A., and Almeida, P. F. F. (2008) A quantitative model for the all-or-none permeabilization of phospholipid vesicles by the antimicrobial peptide cecropin A, *Biophys. J. 94*, 1667–1680.
28. Vaz, W. L. C., and Hallmann, D. (1983) Experimental evidence against the applicability of the Saffman-Delbrück model to the translational diffusion of lipids in phosphatidylcholine bilayer membranes. *FEBS Lett. 152*, 287–290.
29. Bartlett, G. R. (1959) Phosphorous assay in column chromatography. *J. Biol. Chem. 234*, 466–468.
30. Pokorny, A., and Almeida, P. F. F. (2005) Permeabilization of raft-containing lipid vesicles by δ -lysin: A mechanism for cell sensitivity to cytotoxic peptides. *Biochemistry 44*, 9538–9544.
31. Pokorny, A., Yandek, L. E., Elegbede, A. I., Hinderliter, A., and Almeida, P. F. F. (2006) Temperature and composition dependence of the interaction of δ-lysin with ternary mixtures of sphingomyelin/cholesterol/POPC. *Biophys. J. 91*, 2184–2197.
32. Colquhoun, D. (1971) *Lectures on Biostatistics*, Clarendon Press, Oxford, U.K.
33. Colquhoun, D., and Hawkes, A. G. (1987) The interpretation of single channel recordings. In *Microelectrode Techniques. The Plymouth Workshop Handbook* (Ogden, D., Ed.) 2nd ed., pp 141–188, The Company of Biologists Ltd., Cambridge, U.K.
34. Wimley, W. C., and White, S. H. (1996) Experimentally determined hydrophobicity scale of proteins at membrane interfaces. *Nat. Struct. Biol. 3*, 842–848.
35. Hristova, K., and White, S. H. (2005) An experiment-based algorithm for predicting the partitioning of unfolded peptides into phosphatidylcholine bilayer interfaces. *Biochemistry 44*, 12614–12619.
36. Membrane Protein Explorer, http://blanco.biomol.uci.edu/mpex/
37. Ladokhin, A. S., and White, S. H. (2001) Protein chemistry at membrane interfaces: Non-additivity of eletrostatic and hydrophobic interactions. *J. Mol. Biol. 309*, 543–552.
38. Hammond, G. S. (1955) A correlation of reaction rates. *J. Am. Chem. Soc. 77*, 334–338.
39. Nakajima, Y., Qu, X., and Natori, S. (1987) Interaction between liposomes and sarcotoxin IA, a potent antibacterial protein of Sarcophaga peregrina (flesh fly). *J. Biol. Chem. 262*, 1665–1669.
40. Mor, A., and Nicolas, P. (1994) The NH2 -terminal α -helical domain 1–18 of dermaseptin is responsible for antimicrobial activity. *J. Biol. Chem. 269*, 1934–1939.
41. Lee, I. H., Cho, Y., and Lehrer, R. I. (1997) Effects of pH and salinity on teh antimicrobial properties of clavanins. *Infect. Immun. 65*, 2898–2903.
42. Oren, Z., and Shai, Y. (1996) A class of highly potent antibacterail peptides derived from pardaxin, a pore-forming peptide isolated from Moses sole fish Pardachirus marmoratus. *Eur. J. Biochem. 237*, 303–310.
43. Shalev, D. E., Mor, A., and Kustanovich, I. (2002) Structural consequences of carboxyamidation of dermaseptin S3. *Biochemsitry 41*, 7312–7317.
44. Schibli, D., Nguyen, L. T., Kernaghan, S. D., Rekdal, O., and Vogel, H. J. (2006) Structure-function relationships between antimicrobial activities, model membrane interactions, and their micelle-bound NMR structures. *Biophys. J. 91*, 4413–4426.
45. Dathe, M., Schumann, M., Wieprecht, T., Winkler, A., Beyermann, M., Krause, E., Matsuzaki, K., Murase, O., and Bienert, M. (1996) Peptide helicity and membrane surface charge

modulate the balance of electrostatic and hydrophobic interactions with lipid bilayers and biological membranes. *Biochemistry 35*, 12612–12622.

46. Zelezetsky, I., Pacor, S., Pag, U., Papo, N., Shai, Y., Sahl, H.-G., and Tossi, A. (2005) Controlled alteration of the shape and conformational stability of α -helical cell-lytic peptides: Effect on the mode of action and cell specificity. *Biochem. J. 390*, 177–188.
47. Matsuzaki, K., Nakamura, A., Murase, O., Sugishita, K.-i., Fujii, N., and Miyajima, K. (1997) Modulation of magainin 2-lipid bilayer interactions by peptide charge. *Biochemistry 36*, 2104–2111.
48. Dathe, M., Nikolenki, H., Meyr, J., Beyermann, M., and Bienert, M. (2001) Optimization of the antimicrobial activity of magainin peptides by modification of charge. *FEBS Lett. 501*, 146–150.
49. Giangaspero, A., Sandri, L., and Tossi, A. (2001) Amphipathic α -helical antimicrobial peptides: A systematic study of the effects of structural and physical properties on biological activity. *Eur. J. Biochem. 268*, 5589–5600.
50. Mitchell, D. J., Kim, D. T., Steinman, L., Fathman, G. C., and Rothbard, J. B. (2000) Polyarginine enters cells more efficiently than other polycationic homopolymers. *J. Pept. Res. 56*, 318–325.
51. Futaki, S., Suzuki, T., Ohashi, W., Yagami, T., Tanaka, S., Ueda, K., and Sugiura, Y. (2001) Arginine-rich Peptides: An abundant source of membrane-permeable peptides having potential as carriers for intracellular protein delivery. *J. Biol. Chem. 276*, 5836–5840.

BI702205R